

Quest for IR-Pumped Reactions in Dihydrogen-Bonded Complexes

Simona Marincean and James E. Jackson*

Department of Chemistry, Michigan State University, East Lansing, Michigan 48824

Received: March 29, 2004

As possible substrates for one-photon infrared-pumped reaction (IRPR), the structures and decomposition paths of complexes between AlH_4^- and three proton donors, H_2O , HF , and HCl , have been studied by ab initio methods. In each case only one transition state was found for the proton-transfer and H_2 -loss process. For each cluster, the geometry and energy characteristics of reactants, complex, transition state, and products were analyzed with $[\text{AlH}_4 \cdots \text{HCl}]^-$ emerging as the best IRPR candidate. The MP2//6-311++G**-calculated intrinsic reaction coordinate (IRC) confirmed the one-step proton transfer and H_2 loss with no intermediate. Classical trajectories were calculated on the ab initio potential-energy surface, beginning from a large number of initial conditions. With zero-point vibrational energies ($\text{ZPVE} = 1/2h\nu_i$) assigned to all normal modes, based on their calculated harmonic frequencies, ν_i , one or more additional excitation quanta were added to modes associated with Cl-H and Al-H stretching. Proton transfer from HCl and loss of H_2 were calculated to occur on the femtosecond time scale when stretching modes involving the dihydrogen-bonded hydrogens were excited. However, many vibrational oscillations take place before H_2 release. Analysis of the dynamics in terms of the complex's normal modes indicates that the excitation in the reaction-relevant modes remains localized on a time scale > 1 ps.

Introduction

The notion of selective bond cleavage via vibrational activation ("molecular scissors") has long been recognized as a natural corollary to the identification of infrared absorption bands with molecular functional groups. In principle, deposition of sufficient vibrational energy into a chemical bond's stretching mode should induce its rupture, resulting in an infrared-pumped reaction (IRPR). However, many vibrational quanta are needed to break a typical bond, so this idea was not seriously considered until the advent of pulsed lasers, light sources intense enough to accomplish rapid multiphoton excitation.¹ Unfortunately, though lasers have been crucial in the development of today's understanding of molecular dynamics, the main result is the knowledge that the time scales for multiphoton absorption and, most importantly, vibrational relaxation are typically much faster than for any intended reaction. The challenge to those who would design IRPRs is thus clear: the reaction time must be competitive with the relaxation time of the vibrational mode in question, the energy deposited must of course be adequate to surmount the activation barrier (including thermal and tunneling contributions) for the process, and the overall reaction should be irreversible or at least exothermic (i.e., the back reaction should have a high barrier). This paper uses ab initio methods to explore a class of candidate reaction systems that appear to meet these requirements.

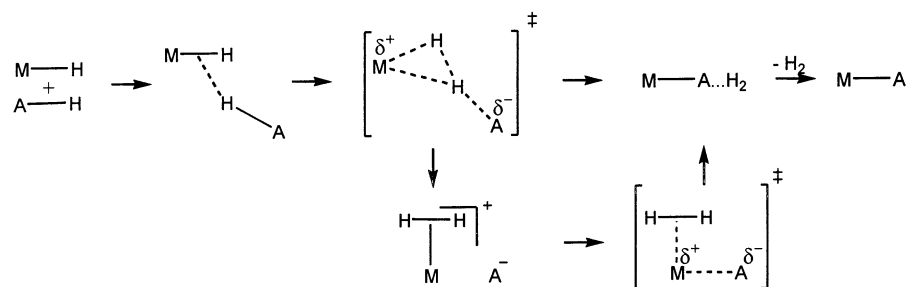
Dihydrogen-bonded complexes $\text{A-H} \cdots \text{H-M}$ ($\text{A} = \text{O}, \text{N}$, halogen; $\text{M} = \text{metal}$) offer several attractive features which should make them good substrates for reaction via single-photon infrared excitation. As in any $\text{A-H} \cdots \text{B}$ hydrogen bond, the A-H stretch vibrations are typically isolated at the high-energy end of the IR spectrum, in the $3000\text{--}4000\text{ cm}^{-1}$ range (i.e., ca.

$8\text{--}12\text{ kcal/mol}$), and are preorganized to align the corresponding normal mode motions with the reaction coordinate for proton transfer. Also, a range of potential-energy surface behaviors is possible; depending on the components' relative acid/base strengths, the complex dissociation energies become larger while the barrier to proton transfer decreases. Unique to the hydridic-to-protonic class of hydrogen bonds, proton transfer from A-H to H-M triggers irreversible loss of H_2 and new A-M bond formation. The most active atoms in this process are both hydrogens (proton and hydride), light particles capable of quantum mechanical tunneling, which may allow them to move on a time scale competitive with vibrational relaxation.

Pico- and femtosecond studies of classical hydrogen-bond dynamics in solutions such as ethanol⁵ in CCl_4 have yielded several important findings: O-H excitation leads to hydrogen-bond cleavage, predissociation lifetime is strongly dependent on the frequency excited, orientational relaxation occurs on the femtosecond time scale, alcohol concentration plays a major role in the peak's broadening as a result of excitation, and reassociation occurs in picoseconds. Recent studies of methanol in nonpolar solvents have shown evidence for different hydrogen-bond-breaking pathways. The Bakker group noted that excitation of the internal⁶ OH groups in methanol clusters dissolved in CCl_4 led to relaxation via dissociation of the corresponding hydrogen bond with a lifetime of 500 fs.⁷ Fayer et al. observed longer dissociation times, 2–3 ps, for the excitation of non-donating OD stretching of MeOD solution in CCl_4 , and they proposed intramolecular energy redistribution followed by energy transfer into the intermolecular modes.⁸ When they measured the OD relaxation of groups that both donate and accept hydrogen bonds in a MeOD solution in CCl_4 , both mechanisms were observed.⁸ Also, excitation of methanol in Na zeolites led to relaxation via hydrogen-bond breaking but on much slower time scales (~ 10 ps).⁷ In the HCl –ether

* To whom correspondence should be addressed. Phone: 517-355-9715 ext.141. Fax: 517-353-1793. E-mail: marincea@msu.edu, jackson@cem.msu.edu.

SCHEME 1: Overall Reaction



hydrogen-bonded systems, H–Cl excitation led to hydrogen-bond breaking but evidence for proton transfer was not observed.⁹

Halogenated ionic hydrogen bonds in small clusters, $\text{Cl}^- \cdot (\text{H}_2\text{O})_n$, exhibit broadening with increasing cluster size, and when a cluster includes a mixture of ionic and neutral hydrogen bonds, the neutral bond is broken upon excitation.¹⁰ In contrast, for the ionic hydrogen bonds in partially deuterated $\text{NaOH}/\text{H}_2\text{O}$ solution, excitation leads to vibrational relaxation on the picosecond scale and deuteron and/or proton hopping within 100 fs.¹¹ When hydrogen-bonded ionic crystals are excited in infrared hole-burning experiments, a lifetime on the time scale of minutes at low temperature is observed.¹² Taken together, the evidence shows that OH can be selectively excited and that in some cases proton transfer occurs as a result.

Hydridic-to-protonic hydrogen bonds, also known as dihydrogen bonds, are interactions between the electrons of polar M–H σ -bonds, where M is less electronegative than H (M = B, Ga, Ir, Os, Re, Ru) and traditional proton donors.¹³ With $\text{H}\cdots\text{H}$ close contacts in the range 1.6–2.2 Å and $(\text{A})\text{H}\cdots\text{H}-\text{M}$ angles between 130° and 180° , they have strengths comparable with classical hydrogen bonds but differ in that they are able to undergo proton transfer that triggers H_2 loss. We have explored this mode of reaction in a number of solid-state complex materials using ordinary thermal excitation.¹⁴ Of particular relevance is the solid-state kinetic study of $\text{LiBH}_4 \cdot \text{TEA}$ (TEA = triethanolamine; IUPAC name tris(2-hydroxyethyl)amine) in which a barrier of 20 kcal/mol was deduced for the rate-determining initial proton transfer. This value is in good agreement with the activation energy found by Mesmer and Jolly for the solution hydrolysis of BH_4^- in H_2O .¹⁵

As noted in the Introduction, a dihydrogen-bonded complex may offer a uniquely promising opportunity for an IRPR. The $\text{H}\cdots\text{H}$ association preorganizes the system, and the particles involved in dihydrogen bonding, H^+ and H^- , are light and capable of tunneling.¹⁶ Therefore, this reaction may be able to proceed rapidly enough to outpace vibrational energy redistribution, a process that normally occurs much faster than chemical reactions. Previous experimental and ab initio studies¹⁷ on H_3O^- , which can be considered the first member of this class of complexes, showed a barrier for proton transfer of 3.8 kcal/mol. The elegant theoretical work of Scheiner et al.¹⁸ on $\text{H}\cdots\text{H}$ -bonded complexes involving Ru hydrides showed small or no barriers for proton transfer depending on the strength of the proton donor. Given such low barriers, the energy needed to excite the H–A bond stretch should be enough to transfer the proton in a one-photon IRPR. The process may be concerted (one step) or follow a stepwise path via intermediate energy minima; these choices are depicted in Scheme 1.

Because Al belongs to the same group as B and Ga and aluminum hydrides are widely used reducing reagents, we considered that it would be of interest to study AlH_4^- as an

M–H candidate and to model the proton-transfer reaction for dihydrogen-bonded complexes involving AlH_4^- . Three H–A partners have been considered: H–OH, H–F, and H–Cl.

Methods of Calculation

Calculations used the MP2 level of theory and the 6-311++G** basis set available in the GAUSSIAN 94,¹⁹ GAUSSIAN 98,²⁰ and GAMESS²¹ packages. Vibrational analyses were performed to confirm the nature of all stationary points on the PES. Complexes were obtained by optimizing a structure with the hydride and the proton donor initially at large distance. $\text{H}\cdots\text{H}$ contact distances and association energies were used as criteria for a dihydrogen-bonded complex. Association energies were calculated as the difference between the energies of the complexes and the sums of the corresponding free partners' energies, including the zero-point vibrational energy (ZPVE) corrections. Because this level of theory had proven quantitatively successful in estimating halide and borohydride ion–molecule association energies,²² we did not correct for basis set superposition error (BSSE). A relaxed potential energy surface (PES) scan for proton transfer/ H_2 -loss was obtained by stepwise shortening of the proton–hydride distance. The highest energy structure was then optimized to locate a transition state.

Once the most suitable candidate ($[\text{AlH}_4 \cdots \text{HCl}]^-$) for IRPR was found, the intrinsic reaction coordinate (IRC) was traced in order to determine the concerted or stepwise nature of the process. Dynamics studies were then performed with different sets of initial conditions. In the first series the starting point considered was the dihydrogen-bonded complex. The energy corresponding to different numbers of vibrational quanta was given to the modes of interest together with ZPVE to all the other modes. In the second trajectory study, the initial geometry was the optimized transition-state structure from the IRC calculation and 0.25 kcal/mol of kinetic energy was given to the reaction mode in the direction of the reactants (i.e., reverse reaction direction) to initiate the dynamics.

Results and Discussion

1. Reactants, Transition States, and Products. Of the proton donors considered, H_2O , HF, and HCl, all formed dihydrogen-bonded complexes with AlH_4^- , as defined by a $\text{H}\cdots\text{H}$ contact distance < 2.4 Å, the sum of the van der Waals radii. The complexes' geometries are slightly bent, with the $\text{H}(\text{A})-\text{H}(\text{Al})-\text{Al}$ (A = F, Cl) angles falling in the range 140 – 150° . In the $[\text{AlH}_4 \cdots \text{H}_2\text{O}]^-$ complex, Figure 1, both protons from H_2O form dihydrogen bonds; the resulting C_{2v} symmetry, cyclic complex thus has a small value for the $\text{H}(\text{O})-\text{H}(\text{Al})-\text{Al}$ angle, 110.0° .

As expected, the elongation of A–H (A = OH, F, Cl) increases with the acidity of the proton donor and the $\text{H}\cdots\text{H}$ close-contact distances decrease in the same sequence, the smallest value corresponding to the $[\text{AlH}_4 \cdots \text{HCl}]^-$ complex. A

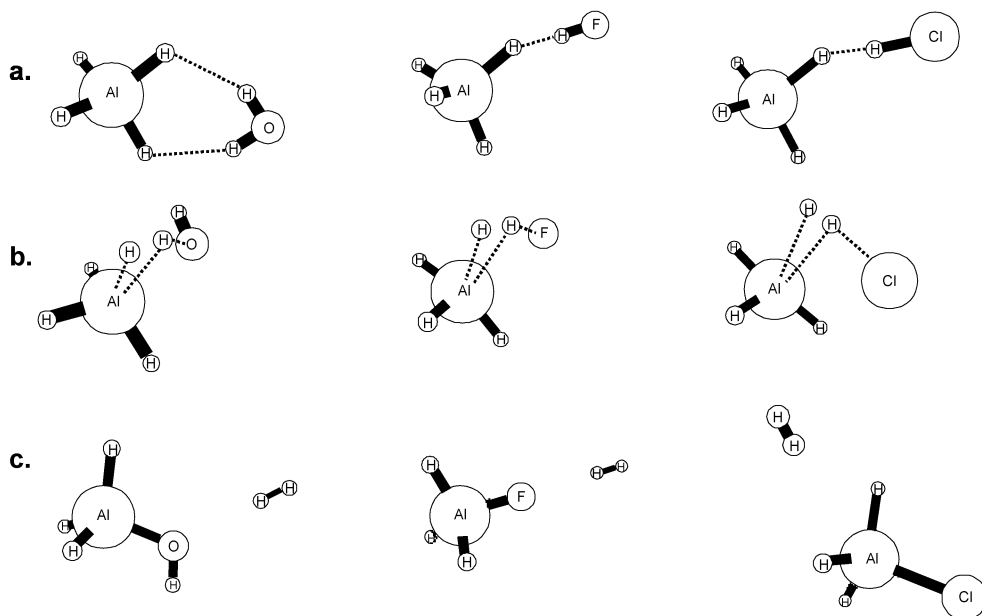


Figure 1. Reactants, transition states, and products for $[\text{AlH}_4\cdots\text{HA}]^-$ systems: (a) reactants; (b) transition states; (c) products.

TABLE 1: Dihydrogen-Bonded Complexes: Geometries (see Figure 1a)

A	H–A ^a		H(A)–H(Al) ^a distance	H(A)–H(Al)–Al ^b angle
	free	complex		
O	0.960	0.967	2.009	110.0
F	0.917	0.956	1.371	143.0
Cl	1.273	1.381	1.226	149.4

^a In Ångstroms. ^b In degrees.

weaker elongation was observed for the H–Al bond involved in dihydrogen bonding together with shrinkage of the other H–Al bonds. These geometry effects are consistent with known experimental structures¹³ and are interpreted as an indication that the interaction is between the electron-deficient hydrogen of H–A and the σ -bonding electrons of the Al–H bond. Table 1 summarizes the relevant geometrical findings. The calculations also reproduce the experimentally observed shift of the A–H stretch to lower frequency upon association, a feature common to most hydrogen-bonded complexes (see Table 2).

The potential-energy surface (PES) for each proton-transfer/hydrogen-loss reaction was initially explored via a relaxed scan from the dihydrogen-bonded complex to the products. In each case, only one maximum was found, suggesting that the reaction occurs via a concerted process. The structure with the highest energy was optimized to a transition state, and a vibrational analysis was performed in order to check the nature of the saddle point. All the transition states have both the proton and hydride in close proximity to the Al at distances in the range of 2.0 Å.²³ As expected, the barrier for proton transfer drops dramatically with decreasing H \cdots H distance in the energy-minimized complex. For all the systems studied the net reaction is strongly exothermic, Table 2, yielding a weakly bound $\text{AlH}_3\text{A}^-\cdots\text{H}_2$ complex, which is calculated to be unstable when zero-point corrections are included.

We judged the $[\text{AlH}_4\cdots\text{HCl}]^-$ complex to be the best candidate for our dynamics studies because it has a proton-transfer barrier, 6.7 kcal/mol, which is within the range of one vibrational quantum for A–H stretching. This activation barrier is also much smaller than the association energy, so that reaction should be preferred over dissociation. Finally, the reverse reaction has a huge barrier, so the reaction is

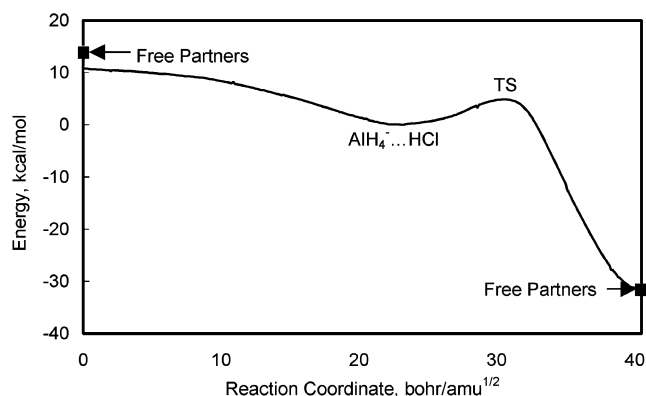


Figure 2. IRC calculation for proton transfer and H_2 loss in $[\text{AlH}_4\cdots\text{HCl}]^-$.

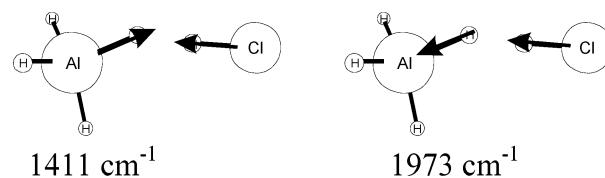


Figure 3. Excited modes.

effectively irreversible. To check that the transition state connects the reactant and products, an intrinsic reaction coordinate (IRC) calculation, in mass-weighted Cartesian coordinates, was performed with the result pointing to a single-step process, Figure 2.

2. Dynamics. Once the reactants, products, and transition-state geometries were located on the PES, the reaction dynamics could be explored via ab initio classical trajectories. Among the modes associated with the dihydrogen-bonded complex, the ones most relevant to proton transfer are 1411 and 1973 cm^{-1} . These modes represent mixtures of symmetrical and antisymmetrical Al–H and Cl–H stretches involved in the H \cdots H interaction.

To model the IRPR of $[\text{AlH}_4\cdots\text{HCl}]^-$, we performed dynamic reaction path (DRP) calculations at the MP2 level.²⁴ A method implemented in the GAMESS package, DRP allows for deposition of selected quantities of energy into specific vibrational

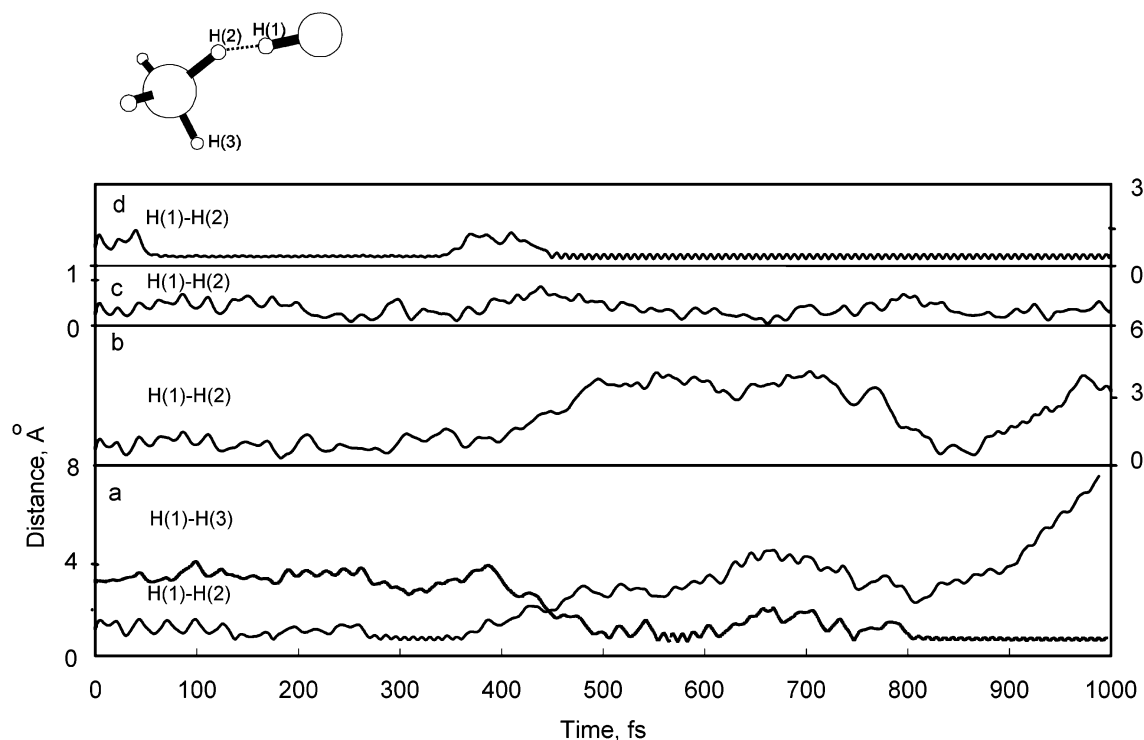


Figure 4. Distance evolution in vibrationally excited complex at 1411 cm^{-1} : (a) $1.5h\nu$, (b) $2.5h\nu$, (c) $3.5h\nu$, and (d) $4.5h\nu$ excitation energy.

TABLE 2: Energetics of Proton-Transfer Reactions for Dihydrogen-Bonded Complexes

A	$\Delta E_{\text{assoc}}^a$ $\text{AlH}_4^- \cdots \text{HA}$		ΔE_a^a		ΔE_{rxn}^a		$\Delta E_{\text{assoc}}^a$ $\text{AlH}_3\text{A}^- \cdots \text{H}_2$		H–A vibration ^b	
	without ZPVE	with ZPVE	without ZPVE	with ZPVE	without ZPVE	with ZPVE	without ZPVE	with ZPVE	free	complex
OH	12.4	10.1	30.1	27.5	13.5	16.5	2.3	0.5	3884; 4003	3799; 3849
F	17.3	15.5	19.6	18.4	27.1	29.1	2.0	0.3	3325	2200
Cl	15.0	13.9	4.9	6.7	31.3	31.4	1.0	−0.3	3087	1978

^a In kcal/mol. ^b In cm^{-1} .

modes of the complex and classical treatment of the resulting reaction dynamics, i.e., calculation of trajectories, via propagation of the equations of motion on the ab initio potential-energy surface.

The Al–H stretch, 1411 cm^{-1} , was excited with different energies in the range 1.5–4.5 quanta, corresponding to 6.4–19.2 kcal/mol, and all the other modes were given the ZPVE energy, i.e., for i th mode an energy of $1/2h\nu_i$. It is important to note that if the zero-point component of the mode is included, even at the lowest excitation level, the 6.4 kcal/mol of kinetic energy in the proton-transfer mode is close to the activation barrier, 6.7 kcal/mol, while in all the other situations we explored the energy deposited is well above the activation barrier. The time evolution of the H(1)–H(2) distance, where H(1) and H(2) represent, respectively, the proton and hydride involved in dihydrogen bonding, is depicted in Figure 4. For the 1.5 and 4.5 quantum cases the proton transfer is followed by loss of the H_2 molecule within 400–800 fs via assistance from Cl^- . The differences reside in the time scale for proton transfer and in the hydridic hydrogen atom that participates in the process.

While for 4.5 quanta, the particles that react are the ones that are dihydrogen bonded initially, for 1.5 quanta, the AlH_4^- fragment rotates, moving a different hydride into position to interact with the proton and react to form H_2 , Figure 4. For the intermediate energies, 2.5 and 3.5 quanta, the proton is transferred but undergoes reversion without liberation of H_2 over the 1 ps period studied.

The H–Cl stretch, 1973 cm^{-1} , was excited with energies in the range 1.5–3.5 quanta, 9.0–22 kcal/mol, Figure 5. In all

calculations proton transfer was found with the formation of complexed H_2 for time intervals that increased in length with decreasing excitation energy. Only for 3.5 quanta, i.e., 22 kcal/mol, was irreversible H_2 loss accomplished within 200 fs. It is worth noting that proton transfer occurred in all simulations, for both 1411 and 1973 cm^{-1} modes.

It is of importance to know the extent of the reactant vibrational modes' involvement in the proton-transfer/ H_2 -loss reaction. To investigate this aspect, we performed a DRP calculation in which the starting point was the transition state with 0.25 kcal/mol of energy deposited into the imaginary mode.

The amplitude and momentum of the atomic displacements were mapped onto the normal modes of the dihydrogen-bonded complex. In other words the normal modes of the reactant were employed as basis vectors to describe the reaction dynamics. As shown in Figure 6, the modes that we associate with proton transfer, 1411 and 1973 cm^{-1} , appeared to move together, showing significant displacement with an oscillation period of ~ 400 fs ($\sim 80\text{ cm}^{-1}$), evidence of their involvement in the process. These vibrations, however, were not centered about the origin, and several attempts to center them via careful realignment of active and reference structures failed.²⁵ The cause of this offset may be the rotation and bending of the complex as it descends on the PES from the transition state to the dihydrogen-bonded complex minimum. Indeed, the rotation and bending modes showed large amplitudes, as seen in Figure 7.

Mapping the reaction's atom displacements onto the reference stationary point's normal modes is more problematic than originally hoped. Defined as they are as displacement vectors

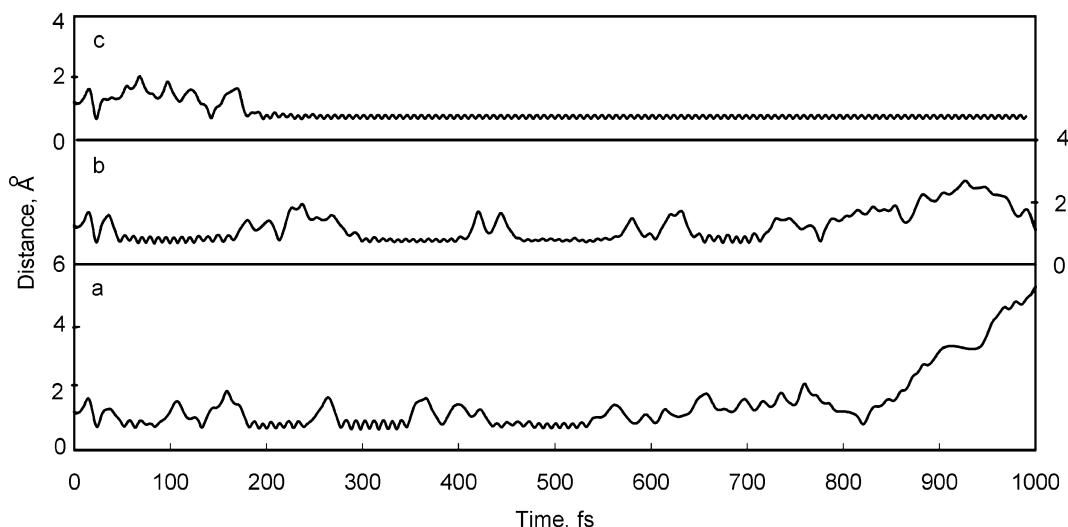


Figure 5. H(1)–H(2) distance evolution in vibrationaly excited complex at 1973 cm^{-1} : (a) $1.5h\nu$, (b) $2.5h\nu$, and (c) $3.5h\nu$ excitation energy.

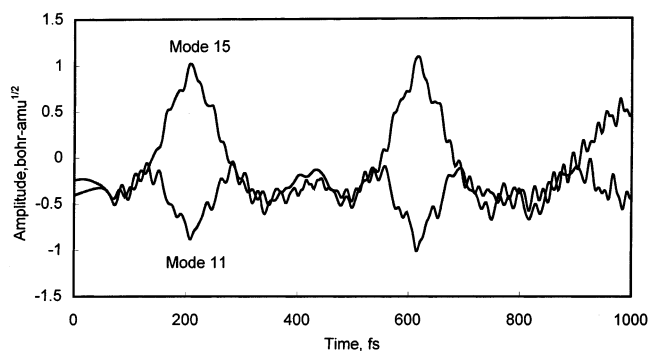


Figure 6. Evolution of modes 11 (1411 cm^{-1}) and 15 (1973 cm^{-1}) upon transition state relaxation.

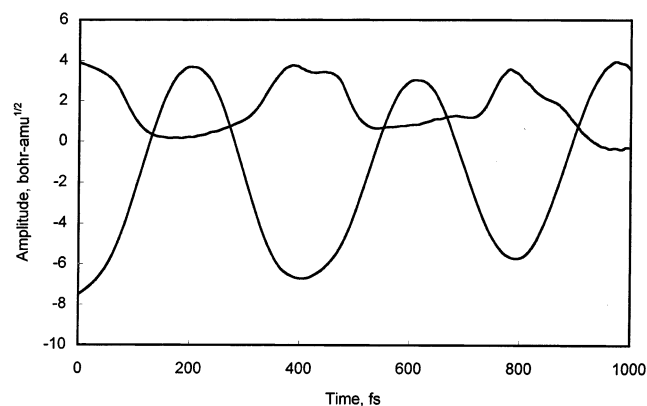


Figure 7. Evolution of selected rotation and bending modes upon transition state relaxation.

in a Cartesian coordinate system, the reference normal modes do not adequately accommodate rotations of either the overall structure or internal fragments. Thus, in the substantial structural reorganizations that occur during reaction in this polyatomic, multiply degenerate, no-symmetry system, the significance of the original modes is quickly lost. A natural alternative might be use of internal coordinate-based normal modes, but the degeneracy problem would remain in the present chemical system.

Overall, the complexity of our system and the state of development of the available software allow only broad interpretation of the reaction in terms of the normal-mode mapping approach.

Additional trajectories need to be computed in this 15-dimensional phase space, but the rapid geometry and momentum changes require small step sizes and consequentially long computational times (typically around 2 weeks of CPU time), which do not readily allow for efficient collection of statistically significant numbers of runs. However, the surprisingly general occurrence of proton transfer (albeit not always leading to dissociation of H_2) is very encouraging for the potential of systems such as these for IRPR. It must be recalled that these simulations are all classical. Presumably the contribution of tunneling would only serve to further enable the reaction. For a more complete understanding we hope soon to be able to compute ab initio trajectories in which the hydride and proton benefit from a quantum mechanical treatment, based on a new formalism²⁶ that will shortly be available in the GAMESS package.²⁷

Conclusions

AlH_4^- is able to form $\text{H}\cdots\text{H}$ bonds with the proton donors H_2O , HF , and HCl in the gas phase. Upon excitation of the modes associated with proton transfer in the $\text{AlH}_4^-\cdot\text{HCl}$ complex, the reaction was driven at larger energies than the barrier for proton transfer. The proton transfer, reversible or not, is observed in all simulations. Although these results need to be refined by consideration of numerous additional trajectories from different starting conditions, and the contributions of quantum mechanical tunneling need to be incorporated in a more rigorous manner, we believe that this initial investigation reveals the promise of such hydridic-to-protonic hydrogen-bonded systems as candidates for bona fide bond-selective infrared pumped reactions.

Acknowledgment. Private communication with Professor S. Hammes-Schiffer is acknowledged. We thank Professor T. Taketsugu for useful discussions and assistance with the DRP and normal-mode mapping code in GAMESS.

Supporting Information Available: The geometries and frequencies for all the reactants, transition state, and products. This material is available free of charge via the Internet at <http://pubs.acs.org>.

References and Notes

- (1) (a) Isenor, N. R.; Richardson, M. C. *Appl. Phys. Lett.* **1971**, *18*, 225. (b) Zewail, A. H. *Phys. Today* **1980**, *33*, 27. (c) Lupo, D. W.; Quack, M. *Chem. Rev.* **1987**, *87*, 181.

- (2) Lewis, R. J.; Rabitz, H. A. *J. Phys. Chem. A* **2002**, *106*, 6427.
- (3) Henriksen, N. E. *Chem. Soc. Rev.* **2002**, *31*, 37.
- (4) Althorpe, S. C.; Fernandez-Alonso, F.; Bean, B. D.; Ayers, J. D.; Pomerantz, A. E.; Zare, R. N.; Wrede, E. *Nature* **2002**, *416*, 67.
- (5) (a) Laenen, R.; Rauscher, C. *J. Chem. Phys.* **1997**, *106*, 8974. (b) Laenen, R.; Rauscher, C.; Laubereau, A. *J. Phys. Chem. A* **1997**, *107*, 3201. (c) Woutersen, S.; Emmerichs, U.; Bakker, H. J. *J. Chem. Phys.* **1997**, *107*, 1483. (d) Laenen, R.; Rauscher, C. *J. Mol. Struct.* **1998**, *115*, 448.
- (6) An "internal OH" in this context means an OH that is involved both as proton donor and proton acceptor in hydrogen bonds at the same time.
- (7) Bonn, M.; Bakker, H. J.; Kleyn, A. W.; van Santen, R. *J. Phys. Chem.* **1996**, *100*, 15301.
- (8) (a) Gaffney, K. J.; Piletic, I. R.; Fayer, M. D. *J. Phys. Chem. A* **2002**, *106*, 9428. (b) Gaffney, K. J.; Davis, P. H.; Piletic, I. R.; Levinger, N. E.; Fayer, M. D. *J. Phys. Chem. A* **2002**, *106*, 12012.
- (9) Giebels, I. A. M. E.; van der Broek, M. A. F. H.; Kropman, M. F.; Bakker, H. J. *J. Chem. Phys.* **2000**, *112*, 5127.
- (10) (a) Ayotte, P.; Bailey, C. G.; Weddle, G. H.; Johnson, M. A. *J. Phys. Chem. A* **1998**, *102*, 3067. (b) Choi, J.-H.; Kuwata, K. T.; Cao, Y.-B.; Okumura, M. *J. Phys. Chem. A* **1998**, *102*, 503.
- (11) Nienhuys, H. K.; Lock, A. J.; van Santen, R. A.; Bakker, H. J. *J. Chem. Phys.* **2002**, *117*, 8021.
- (12) (a) Yu, G.-S.; Li, H.-W.; Strauss, H. L. *J. Phys. Chem. A* **1997**, *101*, 8009. (b) Li, H.-W.; Yu, G.-S.; Strauss, H. L. *J. Phys. Chem. B* **1998**, *102*, 298. (c) Strauss, H. L.; Cha, Y.-H. *J. Phys. Chem. A* **2002**, *106*, 3531.
- (13) (a) Crabtree, R. H.; Siegbahn, P. E. M.; Eisenstein, O.; Rheingold, A. L.; Koetzle, T. F. *Acc. Chem. Res.* **1996**, *29*, 348. (b) Crabtree, R. H. *J. Organomet. Chem.* **1998**, *577*, 111. (c) Shubina, E. S.; Belkova, N. V.; Epstein, L. M. *J. Organomet. Chem.* **1997**, *536*, 17. (d) Alkorta, I.; Rozas, I.; Elguero, J. *Chem. Soc. Rev.* **1998**, *27*, 163. (e) Crabtree, R. H. *Science* **1998**, *282*, 2000. (f) Crabtree, R. H.; Eisenstein, O.; Sini, G.; Peris, E. *J. Organomet. Chem.* **1998**, *567*, 7. (g) Kelly, P.; Loza, M. *Chem. Br.* **1999**, *35*, 26.
- (14) (a) Custelcean, R.; Jackson, J. E. *J. Am. Chem. Soc.* **1927**, *49*, 12935. (b) Custelcean, R.; Jackson, J. E. *Angew. Chem., Int. Ed. Engl.* **1999**, *38*, 1661. (c) Custelcean, R.; Jackson, J. E. *J. Am. Chem. Soc.* **2000**, *122*, 5251. (d) Custelcean, R.; Vlassa, M.; Jackson, J. E. *Angew. Chem., Int. Ed.* **2000**, *39*, 3299. (e) Custelcean, R.; Jackson, J. E. *Chem. Rev.* **2001**, *101*, 1963.
- (15) Mesmer, R. E.; Jolly, W. L. *Inorg. Chem.* **1962**, *1*, 608.
- (16) (a) Limbach, H.-H.; Scherer, G.; Maurer, M.; Chaudret, B. *Angew. Chem., Int. Ed.* **1992**, *31*, 1369. (b) Bahnson, B. J.; Park, D.-H.; Kim, K.; Plapp, B. V.; Klinman, J. P. *Biochemistry* **1993**, *32*, 5503. (c) Kim, T.-G.; Lee, S.-I.; Jang, D.-J. *J. Phys. Chem.* **1995**, *99*, 12698. (d) Kohen, A.; Cannio, R.; Bartolucci, S.; Klinman, J. P. *Nature* **1999**, *399*, 496. (e) Karsten, W. E.; Hwang, C.-C.; Cook, P. F. *Biochemistry* **1999**, *38*, 4398. (f) Kohen, A.; Klinman, J. P. *Acc. Chem. Res.* **1998**, *31*, 397. (g) Truhlar, D. G.; Gao, J.; Alhambra, C.; Garcia-Viloca, M.; Corchado, J.; Sanchez, M. L.; Villa, J. *Acc. Chem. Res.* **2002**, *35*, 341. (h) Yu, W.-S.; Cheng, C.-C.; Chang, C.-P.; Wu, G.-R.; Hsu, C.-H.; Chou, P.-T. *J. Phys. Chem. A* **2002**, *106*, 8006.
- (17) (a) de Beer, E.; Kim, E. H.; Neumark, D. M.; Gunion, R. F.; Lineberger, W. C. *J. Phys. Chem.* **1995**, *99*, 13627. (b) Miller, T. M.; Viggiano, A. A.; Stevens Miller, A. E.; Morris, R. A.; Henchman, M.; Paulson, J. F.; Van Doren, J. M. *J. Chem. Phys.* **1994**, *100*, 5706.
- (18) Kar, T.; Orlova, G.; Scheiner, S. *J. Phys. Chem. A* **1999**, *103*, 514.
- (19) Frisch, M. J.; Trucks, G. W.; Schlegel, H. B.; Gill, P. M. W.; Johnson, B. G.; Robb, M. A.; Cheeseman, J. R.; Keith, T. A.; Peterson, G. A.; Montgomery, J. A.; Raghavachari, K.; Al-Laham, M. A.; Zakrzewski, V. G.; Ortiz, J. V.; Foresman, J. B.; Cioslowski, J.; Stefanov, B. B.; Nanayakkara, A.; Challacombe, M.; Peng, C. Y.; Ayala, P. Y.; Chen, W.; Wong, M. W.; Andres, J. L.; Replogle, E. S.; Gomperts, R.; Martin, R. L.; Fox, D. J.; Binkley, J. S.; Defrees, D. J.; Baker, J.; Steward, J. P.; Head-Gordon, M.; Gonzales, C.; Pople, J. A. *Gaussian 94* (Revision D.3); Gaussian, Inc.: Pittsburgh, PA, 1995.
- (20) Frisch, M. J.; Trucks, G. W.; Schlegel, H. B.; Scuseria, G. E.; Robb, M. A.; Cheeseman, R.; Zakrzewski, J. R. V. G.; Montgomery, J. A., Jr.; Stratmann, R. E.; Burant, J. C.; Dapprich, S.; Millam, J. M.; Daniels, A. D.; Kudin, K. N.; Strain, M. C.; Farkas, O.; Tomasi, J.; Barone, V.; Cossi, M.; Cammi, R.; Mennucci, B.; Pomelli, C.; Adamo, C.; Clifford, S.; Ochterski, J.; Petersson, G. A.; Ayala, P. Y.; Cui, Q.; Morokuma, K.; Salvador, P.; Dannenberg, J. J.; Malick, D. K.; Rabuck, A. D.; Raghavachari, K.; Foresman, J. B.; Cioslowski, J.; Ortiz, J. V.; Baboul, A. G.; Stefanov, B. B.; Liu, G.; Liashenko, A.; Piskorz, P.; Komaromi, I.; Gomperts, R.; Martin, R. L.; Fox, D. J.; Keith, T.; Al-Laham, M. A.; Peng, C. Y.; Nanayakkara, A.; Challacombe, M.; Gill, P. M. W.; Johnson, B.; Chen, W.; Wong, M. W.; Andres, J. L.; Gonzalez, C.; Head-Gordon, M.; Replogle, E. S.; Pople, J. A. *Gaussian 98* (Revision A.11.1); Gaussian, Inc.: Pittsburgh, PA, 2001.
- (21) Schmidt, M. W.; Baldrige, K. K.; Boatz, J. A.; Elbert, S. T.; Gordon, M. S.; Jensen, J. J.; Koseki, S.; Matsunaga, N.; Nguyen, K. A.; Su, S.; Windus, T. L.; Dupuis, M.; Montgomery, J. A. *J. Comput. Chem.* **1993**, *14*, 1347.
- (22) Jackson, J. E. Unpublished MP2/6-311++G** calculations.
- (23) Previous calculations at the CCSD(T)/TZ2P(f,d) level done by Schleyer et al. concluded that AlH₅ is a weak complex between alane (AlH₃) and a slightly elongated H₂ molecule with an association energy of 1.7 kcal/mol at 0 K. At room temperature AlH₅ was found to be unstable toward dissociation by 3.1 kcal/mol; evidently formation of the weak tricentric bond barely perturbs the 104 kcal/mol H–H bond strength, consistent with the high (22 kcal/mol) barrier calculated for scrambling between H₂ and AlH₃ hydrogens. See Schreiner, P. R.; Schaefer, H. F.; Schleyer, P. von Rague *J. Chem. Phys.* **1995**, *103*, 5565.
- (24) (a) Taketsugu, T.; Gordon, M. S. *J. Phys. Chem.* **1995**, *99*, 8462. (b) Taketsugu, T.; Gordon, M. S. *J. Phys. Chem.* **1995**, *99*, 14597. (c) Taketsugu, T.; Gordon, M. S. *J. Chem. Phys.* **1995**, *103*, 10042.
- (25) We are grateful to Professor T. Taketsugu for patient explanations and several Gamess patches, which made these normal mode mapping procedures possible.
- (26) Webb, S. P.; Iordanov, T.; Hammes-Schiffer, S. *J. Chem. Phys.* **2002**, *117*, 4106.
- (27) Private communication with Professor S. Hammes-Schiffer.